Published in final edited form as:
Nanotechnology. 2009 May 6; 20(18): 185101. doi:10.1088/0957-4484/20/18/185101.

Reverse DNA translocation through a solid-state nanopore by magnetic tweezers

Hongbo Peng[1] and **Xinsheng Sean Ling**
Department of Physics, Brown University, Providence, RI 02912, USA

Abstract

Voltage-driven DNA translocation through nanopores has attracted wide interest for many potential applications in molecular biology and biotechnology. However, it is intrinsically difficult to control the DNA motion in standard DNA translocation processes in which a strong electric field is required in drawing DNA into the pore, but it also leads to uncontrollable fast DNA translocation. Here we explore a new type of DNA translocation. We dub it 'reverse DNA translocation', in which the DNA is pulled through a nanopore mechanically by a magnetic bead, driven by a magnetic-field gradient. This technique is compatible with simultaneous ionic current measurements and is suitable for multiple nanopores, paving the way for large scale applications. We report the first experiment of reverse DNA translocation through a solid-state nanopore using magnetic tweezers.

1. Introduction

Since Kasianowicz *et al* [1] demonstrated voltage-driven DNA translocation through a biological protein nanopore (α-hemolysin) in 1996, there are growing interests in applying nanopores as sensors for rapid analysis of biomolecules (DNA, RNA, protein, etc) [1–18], or interactions between these biomolecules [19,20]. Application of nanopore for low-cost DNA sequencing [21–25] is particularly attractive as there is great need for reducing the cost of sequencing a whole human genome [26]. There are also suggestions [27] on how voltage-driven DNA translocation may be used as part of artificial cells for addressing fundamental processes in molecular biology.

A key issue in the field of nanopore technology is how to control the DNA translocation processes [1,25]. This was first pointed by Kasianowicz *et al* [1]. In the studies using α-hemolysin pores [1,3,4], it was known that a strong electric field is needed to draw a DNA into the pore, by overcoming the entropic barrier of the DNA molecule. However, once a DNA molecule is captured into the pore, the same intense electric field also leads to a high speed of translocation. In experiments using α-hemolysin pores, the speed of translocation is about 1 base μs^{-1} at 120 mV. For solid-state nanopores [7–9,11,18,19,28,29], the translocation speed is faster due to a weaker DNA–pore interaction in typically larger pores, about 25 bases μs^{-1} [7,11] at 120 mV. For 25 bases μs^{-1}, the required electronic bandwidth for single-base detection is 25 MHz at which the electronic noise far exceeds the minute signals that one may expect from differentiating one part of the DNA to another in various proposals of nanopore technology. Thus a technique for slowing down the DNA translocation in a controllable way and applicable to large number of nanopores simultaneously is critical for the nanopore technology.

[1]Current address: IBM T J Watson Research Center, PO Box 218, Yorktown Heights, NY 10598, USA.

There have been encouraging developments in the studies of controlling DNA translocation processes. An interesting approach, that is easily scalable to large number of nanopores, is to increase the viscosity of the buffer solution [31]. With this approach, a speed of 3 bases μs^{-1} has been obtained for a solid-state nanopore [31]. By using an electronic trigger circuit, Bates and coworkers [32] were able to trap a DNA molecule inside the pore by lowering promptly the applied voltage once the DNA enters the pore. However, increasing the viscosity of the buffer or reducing voltage bias across the nanopore also reduces the ionic current signal. A more promising approach is to introduce a separate DNA manipulation mechanism, such as attaching the DNA to a bead and using an optical tweezers to control the bead position. This was accomplished by Keyser *et al* [33,34]. It was demonstrated that one can pull DNA through a solid-state nanopore at a speed of 30 nm s^{-1}, or about 0.0001 bases μs^{-1}.

In this paper, we adopt the DNA-on-bead approach as the basic concept in controlling DNA translocation through a nanopore. Instead of using optical tweezers, we explore the feasibility of using magnetic tweezers. The optical tweezers approach suffers from a number of fundamental difficulties. First it is difficult to scale to large number of nanopores. Second, and more importantly, due to the absorption of laser light by the buffer, the ionic current is coupled with the motion of the optical bead [33,34]. Thus it is difficult to simultaneously measure ionic current while the DNA is being dragged in a dynamic fashion. Here we describe a magnetic tweezers approach that is effective in creating a reverse slow DNA translocation (<0.01 bases μs^{-1} demonstrated) and easily scalable to large number of addressable nanopores [35]. We should also point out that the reverse translocation approach also introduces a new regime of DNA translocation physics that has not been explored theoretically. In standard DNA translocation experiment, the driving force is *localized* at the pore region, extending only over a few nanometers. While in reverse translocation, the driving force is tension which is *extended* over the entire DNA length between the pore and the bead.

The basic concept of the experiment is shown in figure 1. DNA molecules are attached to magnetic beads via the standard streptavidin–biotin bonds. The free end of the DNA can be captured into the nanopore by the applied electric field. Subsequently, one can apply a precisely controlled magnetic force on the magnetic bead to balance the electrical force on the trapped DNA, i.e., the DNA is in a tug-of-war between the magnetic bead and the nanopore. By increasing the magnetic force further, or reducing the bias voltage, until the magnetic force exceeds the electrical force, the DNA can be pulled out of the nanopore from the *cis* side of the nanopore. Since one can construct a magnetic-field gradient over a large space, this technique is inherently applicable to large number of addressable nanopores. By ramping the magnetic field slowly, the DNAs in all the nanopores can be pulled out slowly during one ramping step.

2. Experimental details

2.1. Nanopore device fabrication

The fabrication of the nanopore chips starts with a 500 μm thick (100) Si wafer. First, 20 nm thick Si_3N_4 films are deposited on both sides of Si wafer using low-pressure chemical vapor deposition (LPCVD). Next, a 200 nm thick SiO_2 film is deposited on one side of the wafer (we define it as the front side) by plasma enhanced chemical vapor deposition (PECVD). 600 nm Si_3N_4 layers are deposited on both sides of the wafer using LPCVD. A square window of 774 μm size is opened into the Si_3N_4 layer on the back side by reactive ion etching (RIE). A 200 μm × 200 μm freestanding membrane is then obtained by etching the silicon from the square window on the bask side in KOH (45% w/w at 85 °C). An array of circular regions of 4 μm diameter in the freestanding membrane are thinned down to 20 nm by removing the top two layers (600 nm Si_3N_4/200 nm SiO_2) on the front side of the wafer using RIE and hydrofluoric acid (only one is shown in the figure). 20 nm SiO_2 is deposited onto both sides of the 20 nm

thick membrane using PECVD. A single nanopore is drilled in a transmission electron microscope by focusing the electron beam onto one of the 60 nm thick $SiO_2/Si_3N_4/SiO_2$ circular regions.

2.2. DNA-bead constructs

The λ-phage DNA was purchased from Promega Corporation. The λ-DNAs were biotinylated using the standard protocol [36], by annealing a complementary primer containing a biotin molecule (Invitrogen) onto the 3′ overhang of a λ-DNA, followed by incubation with T4 DNA ligase (New Eng-land Biolabs). The biotinylated λ-DNAs were then mixed with streptavidin-coated magnetic beads (diameter 2.8 μm, Dynabeads M-280 or M-270 from Invitrogen, with average saturation magnetic moment 1.42×10^{-13} A m^2 [37]) in the binding buffer (Invitrogen) at a ratio of 6 pmol λ-DNA per mg of beads. The mixture was incubated at room temperature for 3 h. After the washing step, the beads were suspended in the measurement buffer containing 0.1 M KCl in 10 mM Tris-HCl, 1 mM EDTA buffer (pH = 8.0) and 0.1% Tween 20 (Sigma Aldrich).

2.3. Magnetic tweezers design, fluidic cell design, and ionic current measurement

As sketched in figure 2(a), two 1 inch cubic neodymium iron boron magnets were used to assemble the magnetic tweezers. Two 0.5 inch high wedge shape iron–vanadium–cobalt soft alloy (Hiperco Alloy 50A, Scientific Alloys, Inc., Westerly, RI) were used to focus the magnetic field to a 2 mm gap. The seal between the nanopore chip, of size 5 mm × 5 mm, and the glass slide was established via Norland UV Curing Adhesives. Magnetic beads (Dynabeads M-280 or M-270) were coated with double-strand λ-phage DNAs and then loaded to the upper chamber of the flow cell with 0.1 M KCl, 10 mM Tris-HCl, 1 mM EDTA buffer (pH = 8.0) and 0.1% Tween 20 (Sigma Aldrich). Tween 20 was used to prevent the sticking of magnetic bead to the surface of nanopore chip. The lower chamber was also filled with the same buffer. A voltage bias was applied to the two chambers across the nanopore chip with two Ag/AgCl electrodes. The voltage and ionic current were recorded with Heka EPC 7 plus patch clamp and digitizer Digidata 1322A with low-pass filter at 1 kHz and sampling rate at 20 kHz. To ensure that the features observed in the temporal traces of ionic current through a nanopore were indeed correlated with the position changes of the magnetic bead, a Sony SSC-M374 CCD camera and an Olympus Splan 50× long working distance objective were used to monitor the DNA-bead and the nanopore membrane in real time. A video image of nanopore membrane and DNA-coated magnetic beads is shown in figure 2(b).

3. Results and discussion

3.1. Multiple DNAs captured into the nanopore and breakage of streptavidin–biotin bond

It is known [30,38–40] that the presence of a DNA in a nanopore has two competing effects for the nanopore conductance: the physical volume of the DNA leads to a reduction in total ion population in the nanopore, thereby reducing nanopore conductance; the negatively charged DNA brings in extra counterions, leading to a conductance enhancement. The net effect of a translocating DNA on the nanopore conductance depends on the ionic strength of the buffer solution. In the case of low ionic strength buffer, at 0.1 M KCl used in this experiment, a DNA capture event is indicated as an increase of the ionic current [30,38–40].

We observed two undesired effects: multiple DNAs captured into the nanopore and breakage of streptavidin–biotin bond. Figure 3(a) shows time trace of ionic current through a 20 nm nanopore at 200 mV bias and 0.1 M KCl. When a DNA-coated magnetic bead is around the nanopore, we see a current increase, shown in the left panel of figure 3(a), indicating that a DNA is captured into the nanopore. In our control experiments (data not shown), a magnetic bead without DNA attached does not induce a change in nanopore conductance even when it

is placed on top of the nanopore. Clearly the beads are too large to have a blockage effect on a small pore. As shown in figure 3(a) (left), for this event, shortly after the increase, the ionic current drops back to the baseline level, indicating the DNA is released from the nanopore. Occasionally, another DNA can be captured before the first captured DNA leaves the nanopore. We observed that in many occasions, several (up to 5) DNAs can be captured in a sequential manner. As shown in figure 3(a) (right), four DNAs are captured into a 20 nm nanopore.

We found that the total ionic current increase is linearly proportional to the number of DNAs in the nanopore, as shown in figures 3(b) and (c). This is not surprising since the number of counterions brought into the nanopore is proportional to the number of DNAs inside the nanopore. By summarizing the arguments presented by Chang *et al* [30, 40], Fan *et al* [38] and Smeets *et al* [39], the overall current change due to the entering of one DNA will be:

$$\Delta I=(V/L_{\text{pore}})\,(q/b)\,(1-\varphi)\mu_{\text{KC}} -qM_{\text{KCl}}N_{\text{A}}(V/L_{\text{pore}})\,(\mu_{\text{K}}+\mu_{\text{Cl}})A_{\text{DNA}} \quad (1)$$

where V is the voltage across the nanopore, V/L_{pore} is the electric field inside the nanopore, q is the electric charge, b(=0.17 nm) is the axial distance between successive charges on the DNA chain, $\mu_{\text{KC}}, \mu_{\text{K}}, \mu_{\text{Cl}}$ are mobility of mobile potassium counterion, potassium ion in bulk solution and chloride ion in bulk solution respectively, M_{KCl} is KCl concentration, N_{A} is the Avogadro's number, A_{DNA} is cross-section area of the DNA and $(1-\varphi)$ is the fraction of mobile counterions. If there are N DNAs in the nanopore, the ionic current through the nanopore will be:

$$I=I_{\text{freepore}}+N[\,(V/L_{\text{pore}})\,(q/b)\,(1-\varphi)\mu_{\text{KC}} -qM_{\text{KCl}}N_{\text{A}}(V/L_{\text{pore}})\,(\mu_{\text{K}}+\mu_{\text{Cl}})A_{\text{DNA}}\,] \quad (2)$$

where I_{freepore} is the ionic current when there are no DNAs in the nanopore. The current increases linearly with the number of DNAs in the nanopore.

We can use equation (1) to give an estimate for the ionic current increase when a DNA enters the pore. Assuming L_{pore} = 60 nm, $\mu_{\text{KC}} = \mu_{\text{K}}$, and φ = 0.76 [41], the expected ionic current increase due to DNA entering at 200 mV bias and 0.1 M KCl solution is about 42 pA. In comparison, the measured value is above 200 pA. We suggest two possible causes for this discrepancy. The first is obvious. It is known that the TEM-drilled nanopores have an hourglass shape [42] instead of a simple cylindrical shape as assumed in the equation, and its shape changes with time in the electron beam during TEM drilling and imaging. Thus the effective thickness L_{pore} can vary widely from sample to sample and should be significantly less than 60 nm of the membrane thickness. Secondly, we note that the fraction of mobile counterions $(1-\varphi)$ ranges from $0.12e^{-}$/bp [43, 44] to $1e^{-}$/bp [45] in the published literatures, thus our assumption φ = 0.76 [41] may not hold.

As to the reason that the DNA is released from the nanopore, in figure 3(a), it is unlikely that the entire λ-DNA (48.5 kilobase pairs) can be pulled out of the nanopore by the thermal motion of the bead, considering the facts that the trapping force on the DNA at 200 mV voltage bias is about 48 pN [34], and the energy needed to pull one nucleotide base out of the nanopore is about 108 meV, which is much larger than the thermal activation energy 26 meV at room temperature. The releasing of DNA from the nanopore must be due to the breakage of the DNA from the magnetic bead. The DNA is covalently bonded to a single biotin molecule, the polystyrene shell of the magnetic bead is covalently bonded to streptavidin, and they are linked through the non-covalent streptavidin–biotin bond. So this non-covalent streptavidin–biotin

bond is the weakest link here. Note that Merkel *et al* [46], in their experiment using atomic force microscopy (AFM) for measuring the strength of the streptavidin–biotin bond, have shown that the streptavidin–biotin bond strength ranges from about 5 to 170 pN depending on the loading rate. The estimated force on the DNA is about 48 pN at 200 mV bias [34] in our case, so we believe that the release of DNA from nanopore is due to the breakage of the streptavidin–biotin bond.

For each DNA capturing and releasing event, we extract two parameters: (1) the amplitude of the current change as the event current (when there is a DNA in the nanopore) subtracting the baseline current (empty pore); (2) the DNA capture time as the time delay between the DNA capture and release. Figure 4 shows a scatter plot of the amplitudes of the current changes versus DNA capture times at two different voltage biases 200 mV and 300 mV, respectively. (Note that each magnetic bead can bond to more than 50 000 λ-DNAs [47].) Note that the amplitudes of the current changes, for the cases of 200 and 300 mV, are proportional to the applied voltage biases, which is reasonable. But the time between the DNA capture and release is over a wide range of timescales, from 2 ms to several hundred milliseconds, which is quite different from the standard DNA translocation events, as shown by other groups [7,11,39]. For the standard DNA translocation events [7,11,39], the DNAs are not bonded to any surface and are driven through the nanopore directly by the electrical field in the nanopore. In the configuration of our experiment, the DNAs are attached the magnetic bead by the streptavidin–biotin bonds and the electrical force on the DNA has to break the streptavidin–biotin bonds first before the DNA is free to translocate through the nanopore. Merkel *et al* [46], in their AFM experiment, have shown that the survival time of the streptavidin–biotin bond ranges from about 1 ms to 1 min depending on the force loading rate. The scales of the survival times of streptavidin–biotin bonds, from Merkel *et al* [46], are consistent with what we observed here.

3.2. Reverse DNA translocation using magnetic tweezers

As shown in figure 5, we apply 200 mV voltage bias across the nanopore and then use a hand-held magnet to drag one DNA-coated magnetic bead slowly onto the part of the membrane where a 10 nm nanopore has been drilled roughly at the center (using a TEM). The ionic current increases when a DNA is captured by the nanopore. Once this occurs, the magnetic bead becomes immobile. We confirmed this observation by direct real-time video microscopy using a CCD camera and a long working distance objective. We then lower the bias to 50 mV to avoid breakage of the streptavidin–biotin bond of the captured DNA.

To pull the DNA out of the nanopore mechanically, we use a pair of magnetic tweezers shown in figure 2(a). For fine-tuning the magnetic force on the bead, the magnets are mounted on a Burleigh Inchworm nano-positional stage. The gradual increase of magnetic force is achieved by moving the magnets slowly towards the nanopore chip. In the distance range over which the DNA is pulled out, the force increase rate is less than 0.2 fN per step on the Burleigh stage. (The Burleigh stage can move 20 nm per step, and it can traverse at a speed from 0.01 to 2062 μm s^{-1}.) Once the magnetic force exceeds the electric force (at 50 mV), the magnetic bead moves away from the pore region. Coincidentally, the nanopore ionic conductance drops as shown in figure 5, indicating the DNA is released (or pulled out) from the nanopore. We can time the two events to within 33 ms as limited by the frame rate of our CCD video camera Sony SSC-M374.

Although we confirmed that the ionic current drops simultaneously as the magnetic bead is moving away from the nanopore, to further confirm that the rise and fall of the nanopore ionic conductance are indeed corresponding to the capture and release of the same DNA from the nanopore, we compare the change of the ionic conductance of the nanopore during the DNA capture and release. In figure 6(a), the ionic current versus time trace for the DNA capture is

plotted. Respectively, the time trace of the ionic current for the DNA release is shown in figure 6(b). To reduce the systematic errors caused by the slow drift of the baseline current, here we pick about 13 000 data points around each event, spanning over 0.5 s. (The slow drift of baseline current of SiO_2 or Si_3N_4 pores is a well-known but poorly understood phenomenon. It is generally attributed to the surface chemistry [48] of the SiO_2 or Si_3N_4 surfaces in buffer conditions or air bubbles [49] being trapped or released from the surface of the nanopore.) The data was sampled at the same rate and under the same experimental conditions. The data points are binned to the same number of bins, 35, for both traces. The histograms for each current versus time traces are shown in the insets of figure 6. The histograms are then fitted using a sum of two Gaussians. From the fittings, we obtain a current increase of $\Delta I_{\text{capture}} = 0.253 \pm 0.002$ nA (at 200 mV) for DNA capture, and a current decrease $\Delta I_{\text{release}} = 0.062 \pm 0.001$ nA (at 50 mV) for DNA release. The corresponding changes in conductance are $\Delta G_{\text{capture}} = 1.265 \pm 0.01$ nS and $\Delta G_{\text{release}} = 1.24 \pm 0.02$ nS. Within the accuracy of our experiment, we find perfect agreement between the conductance changes corresponding to capture and release of a single DNA in a nanopore.

In figure 7, we zoom into the ionic current trace of DNA being released from the nanopore. The zoom-in ionic current trace reveals that the transit time is about 19 ms. To compare, the histogram of the transit times of the ionic current increase and decrease from 50 sequential DNA events (due to the breakage of the streptavidin–biotin bond as shown in figures 3(a) and 4) is shown in the inset of figure 7. The transit times are less than 2 ms and the histogram peaks at 1.2 ms, which is the 1 kHz cutoff frequency set in our ionic current measurement system. We thus conclude that the 19 ms is the actual time that it takes the end of the DNA to pass through the 60 nm long nanopore channel while it is being put out of the nanopore by the magnetic bead. As such, the speed of the end of the DNA moving out of the nanopore can be estimated to be about 0.003 16 nm μs^{-1}, or 0.0096 bases μs^{-1}.

It is likely that the speed of reverse DNA translocation may vary in different stages of the translocation. When the end of the DNA is in the nanopore, the net force on the DNA is largest (the magnetic force is largest as the bead is closest to the magnetic tweezers and the entropic force exerted by the random coil part of the DNA is smallest as the DNA has been stretched), so does the instant speed of the DNA. Thus the average speed of the DNA during the pulling-out process should be lower than that of the end of the DNA moving through the nanopore. By comparing our result to those of the standard DNA translocation [7,11], we find that the average speed of the reverse DNA translocation (using magnetic tweezers here) is more than 2000-fold slower.

3.3. Discussion

We wish to highlight the fundamental differences between the basic physics in reverse DNA translocation and in standard translocation. In standard translocation experiment, the driving force is the electrophoretic action of the electric field inside the pore. Thus the driving force is local on the part of the DNA inside the pore. There have been numerous theoretical models and analyses on the effects of DNA–pore interaction [50], and especially, the role of entropy from the random coils of DNA on both sides of the nanopore [51,52]. Here, in reverse DNA translocation, the DNA is held under tension, thus the driving force is extended on the part of DNA that is stretched between the magnetic bead and the nanopore. This allows the possibility of studying the effects of entropic force on DNA translocation when the random coil of the DNA presents at only one side of the nanopore. By calibrating *in situ* the magnetization of each bead and pulling the trapped DNA out of the nanopore at 0 V bias, one should be able to measure the entropic force and explore the dynamics of DNA molecules in nanoscale confinement.

In future applications where multiple nanopores are used simultaneously, DNAs in different nanopores may not be pulled out at the same time. The drag force on each DNA may be different

in different pores due to variations in DNA–pore interaction as a result of inhomogeneity in pore sizes. Nevertheless, since one can ramp the magnetic field and thus the pulling force, one should be able to pull out all DNAs in different pores. We believe that our approach here is inherently suitable for parallel manipulations of DNAs in multiple nanopores.

4. Conclusion

In conclusion, we performed the first reverse DNA translocation experiment using magnetic tweezers. Controlled capture and slow release of DNA from a solid-state nanopore have been demonstrated. Comparing to that of the optical tweezers approach, the scalability of magnetic tweezers approach has its unique advantage and offers optimism for DNA sequencing applications since it is compatible with nanopore arrays devices being developed in many laboratories worldwide.

Acknowledgments

This work was supported in part by a grant from the NSF-NIRT program and by Award Number R21HG004369 from the National Human Genome Research Institute (NHGRI). The content is solely the responsibility of the authors and does not necessarily represent the official views of NSF, NHGRI or NIH. We acknowledge useful discussions with Derek Stein and Ulrich Keyser.

References

1. Kasianowicz JJ, Brandin E, Branton D, Deamer DW. Characterization of individual polynucleotide molecules using a membrane channel. Proc Natl Acad Sci USA 1996;93:13770–773. [PubMed: 8943010]
2. Gu L, Braha O, Conlan S, Cheley S, Bayley H. Stochastic sensing of organic analytes by a pore-forming protein containing a molecular adapter. Nature 1999;398:686–90. [PubMed: 10227291]
3. Akeson M, Branton D, Kasianowicz JJ, Brandin E, Deamer DW. Microsecond timescale discrimination among polycytidylic acid, polyadenylic acid, and polyuridylic acid as homopolymers or as segments within single RNA molecules. Biophys J 1999;77:3227–33. [PubMed: 10585944]
4. Meller A, Nivon L, Brandin E, Golovchenko J, Branton D. Rapid nanopore discrimination between single polynucleotide molecules. Proc Natl Acad Sci USA 2000;97:1079–84. [PubMed: 10655487]
5. Henrickson SE, Misakian M, Robertson B, Kasianowicz JJ. Driven DNA transport into an asymmetric nanometer-scale pore. Phys Rev Lett 2000;85:3057–60. [PubMed: 11006002]
6. Meller A, Nivon L, Branton D. Voltage-driven DNA translocations through a nanopore. Phys Rev Lett 2001;86:3435–8. [PubMed: 11327989]
7. Li J, Gershow M, Stein D, Brandin E, Golovchenko JA. DNA molecules and configurations in a solid-state nanopore microscope. Nat Mater 2003;2:611. [PubMed: 12942073]
8. Heng JB, et al. The detection of DNA using a silicon nanopore. IEDM Tech Digest 2003:767–70.
9. Heng JB, Ho C, Kim T, Timp R, Aksimentiev A, Grinkova YV, Sligar S, Schulten K, Timp G. Sizing DNA using a nanometer-diameter pore. Biophys J 2004;87:2905–91. [PubMed: 15326034]
10. Mathe J, Aksimentiev A, Nelson DR, Schulten K, Meller A. Orientation discrimination of single-stranded DNA inside the α-hemolysin membrane channel. Proc Natl Acad Sci USA 2005;102:12377–82. [PubMed: 16113083]
11. Storm AJ, Storm C, Chen J, Zandbergen H, Joanny JF, Dekker C. Fast DNA translocation through a solid-state nanopore. Nano Lett 2005;5:1193–7. [PubMed: 16178209]
12. Movileanu L, Howorka S, Braha O, Bayley H. Detecting protein analytes that modulate transmembrane movement of a polymer chain within a single protein pore. Nat Biotechnol 2000;18:1091–5. [PubMed: 11017049]
13. Howorka S, Cheley S, Bayley H. Sequence-specific detection of individual DNA strands using engineered nanopores. Nat Biotechnol 2001;19:636–9. [PubMed: 11433274]

14. Vercoutere W, Winters-Hilt S, Olsen H, Deamer D, Haussler D, Akeson M. Rapid discrimination among individual DNA hairpin molecules at singlenucleotide resolution using an ion channel. Nat Biotechnol 2001;19:248–52. [PubMed: 11231558]
15. Mathe J, Visram H, Viasnoff V, Rabin Y, Meller A. Nanopore unzipping of individual DNA hairpin molecules. Biophys J 2004;87:3205–12. [PubMed: 15347593]
16. Sauer-Budge AF, Nyamwanda JA, Lubensky DK, Branton D. Unzipping kinetics of double-stranded DNA in a nanopore. Phys Rev Lett 2003;90:238101. [PubMed: 12857290]
17. Halverson KM, Panchal RG, Nguyen TL, Gussio R, Little SF, Misakian M, Bavari S, Kasianowicz JJ. Anthrax biosensor, protective antigen ion channel asymmetric blockade. J Biol Chem 2005;280:34056–62. [PubMed: 16087661]
18. Fologea D, Ledden B, McNabb DS, Li J. Electrical characterization of protein molecules by a solid-state nanopore. Appl Phys Lett 2007;91:053901.
19. Zhao Q, Sigalov G, Dimitrov V, Dorvel B, Mirsaidov U, Sligar S, Aksimentiev A, Timp G. Detecting SNPs using a synthetic nanopore. Nano Lett 2007;7:1680–5. [PubMed: 17500578]
20. Hornblower B, Coombs A, Whitaker RD, Kolomeisky A, Picone SJ, Meller A, Akeson M. Single-molecule analysis of DNA–protein complexes using nanopores. Nat Methods 2007;4:315–7. [PubMed: 17339846]
21. Lagerqvist J, Zwolak M, Di Ventra M. Fast DNA sequencing via transverse electronic transport. Nano Lett 2006;6:779–82. [PubMed: 16608283]
22. Gracheva ME, Xiong A, Aksimentiev A, Schulten K, Timp G, Leburton JP. Simulation of the electric response of DNA translocation through a semiconductor nanopore–capacitor. Nanotechnology 2006;17:622–33.
23. Soni G, Meller A. A progress towards ultrafast DNA sequencing using solid state nanopores. Clin Chem 2007;53:1996–2001. [PubMed: 17890440]
24. Ling XS, Bready B, Pertsinidis A. Hybridization-assisted nanopore sequencing of nucleic acids. USPTO Patent Application 2006:20070190542.
25. Branton D, et al. The potential and challenges of nanopore sequencing. Nat Biotechnol 2008;26:1146–53. [PubMed: 18846088]
26. National Human Genome Research Institute, Revolutionary Genome Sequencing Technologies. http://grants1.nih.gov/grants/guide/rfa-files/RFAHG-04-003.html
27. Austin R. Nanopores: the art of sucking spaghetti. Nat Mater 2003;2:567. [PubMed: 12951593]
28. Li J, Stein D, McMullan C, Branton D, Aziz MJ, Golovchenko JA. Ion-beam sculpting at nanometre length scales. Nature 2001;412:166–9. [PubMed: 11449268]
29. Storm AJ, Chen JH, Ling XS, Zandbergen HW, Dekker C. Fabrication of solid-state nanopores with single-nanometre precision. Nat Mater 2003;2:537–40. [PubMed: 12858166]
30. Chang H, Kosari F, Andreadakis G, Alam MA, Vasmatzis G, Bashir R. DNA-mediated fluctuations in ionic current through silicon oxide nanopore channels. Nano Lett 2004;4:1551–8.
31. Fologea D, Uplinger J, Thomas B, McNabb DS, Li J. Slowing DNA translocation in a solid-state nanopore. Nano Lett 2005;5:1734–7. [PubMed: 16159215]
32. Bates M, Burns M, Meller A. Dynamics of DNA molecules in a membrane channel probed by active control techniques. Biophy J 2003;84:2366–72.
33. Keyser UF, van der Does J, Dekker C, Dekker NH. Optical tweezers for force measurements on DNA in nanopores. Rev Sci Instrum 2006;77:105105.
34. Keyser UF, Koeleman BN, van Dorp S, Krapf D, Smeets RMM, Lemay SG, Dekker NH, Dekker C. Direct force measurements on DNA in a solid-state nanopore. Nat Phys 2006;2:473–7.
35. Ling XS. Addressable nanopores and micropores including methods for making and using same. USPTO Patent Application 2005:20050127035.
36. Haber C, Wirtz D. Magnetic tweezers for DNA micromanipulation. Rev Sci Instrum 2000;71:4561–70.
37. Amblard F, Yurke B, Pargellis A, Leibler S. A magnetic manipulator for studying local rheology and micromechanical properties of biological systems. Rev Sci Instrum 1996;87:818–27.
38. Fan R, Karnik R, Yue M, Li D, Majumdar A, Yang P. DNA translocation in inorganic nanotubes. Nano Lett 2005;5:1633–7. [PubMed: 16159197]

39. Smeets RMM, Keyser UF, Krapf D, Wu MY, Dekker NH, Dekker C. Salt dependence of ion transport and DNA translocation through solid-state nanopores. Nano Lett 2006;6:89–95. [PubMed: 16402793]
40. Chang H, Venkatesan BM, Iqbal SM, Andreadakis G, Kosari F, Vasmatzis G, Peroulis D, Bashir R. DNA counterion current and saturation examined by a MEMS-based solid state nanopore sensor. Biomed Microdev 2006;8:263–9.
41. Manning GS. The molecular theory of polyelectrolyte solutions with applications to the electrostatic properties of polynucleotides. Q Rev Biophys 1978;11:179–246. [PubMed: 353876]
42. Kim M-JB, McNally KM, Meller A. Characteristics of solid-state nanometer pores fabricated using transmission electron microscope. Nanotechnology 2007;18:205302.
43. Smith S, Bendich A. Electrophoteric charge density and persistence length of DNA as measured by fluorescence microscopy. Biopolymers 1990;29:1167–73. [PubMed: 2369630]
44. Gurrieri S, Smith SB, Bustamante C. Trapping of megabase-sized DNAmolecules during agarose gel electrophoresis. Proc Natl Acad Sci USA 1999;96:453–8. [PubMed: 9892654]
45. Schellman JA, Stigter D. Electrical double layer, zeta potential, and electrophoretic charge of double-stranded DNA. Biopolymers 1977;16:1415–34. [PubMed: 880365]
46. Merkel R, Nassoy P, Leung A, Ritchie K, Evans E. Energy landscapes of receptor–ligand bonds explored with dynamic force spectroscopy. Nature 1999;397:50–3. [PubMed: 9892352]
47. https://www.invitrogen.com
48. Ho C, Qiao R, Heng JB, Chatterjee A, Timp RJ, Aluru NR, Timp G. Electrolytic transport through a synthetic nanometer–diameter pore. Proc Natl Acad Sci USA 2005;102:10445–50. [PubMed: 16020525]
49. Smeets RMM, Keyser UF, Wu MY, Dekker NH, Dekker C. Nanobubbles in solid-state nanopores. Phys Rev Lett 2006;97:088101. [PubMed: 17026338]
50. Lubensky DK, Nelson DR. Driven polymer translocation through a narrow pore. Biophys J 1999;77:1824. [PubMed: 10512806]
51. Sung W, Park PJ. Polymer translocation through a pore in a membrane. Phys Rev Lett 1996;77:783–6. [PubMed: 10062901]
52. Muthukumar M. Translocation of a confined polymer through a hole. Phys Rev Lett 2001;86:3188. [PubMed: 11290139]

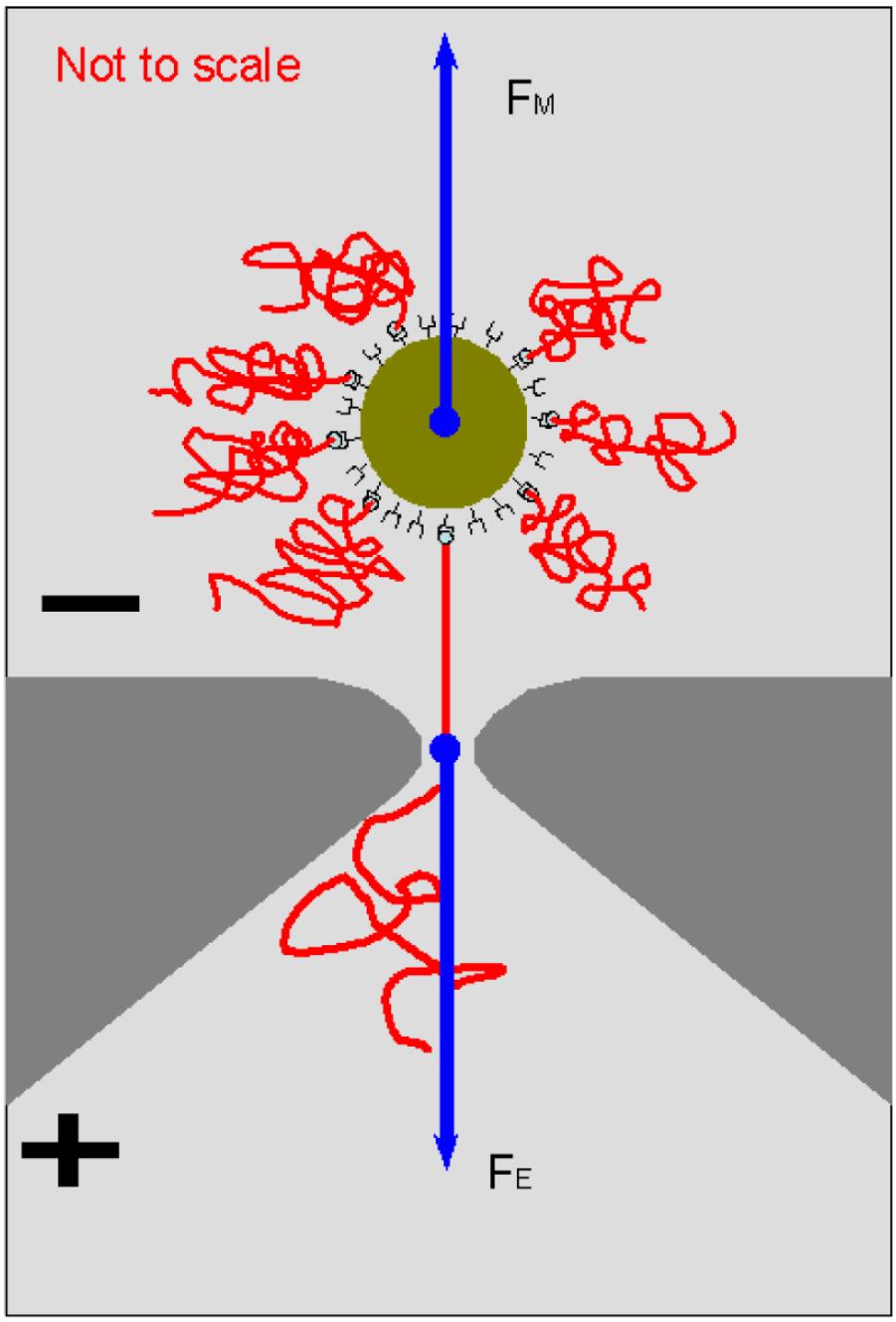

Figure 1.
Schematic of the reverse DNA translocation using magnetic tweezers. Two reservoirs, filled with ionic buffer, are separated by a nanopore chip (shown in gray). A voltage bias is applied across the nanopore chip. DNAs (shown in red) are attached to the magnetic bead via standard streptavidin–biotin bonds. Electrical force F_E on the DNA and magnetic force F_M on the magnetic bead are drawn in blue.

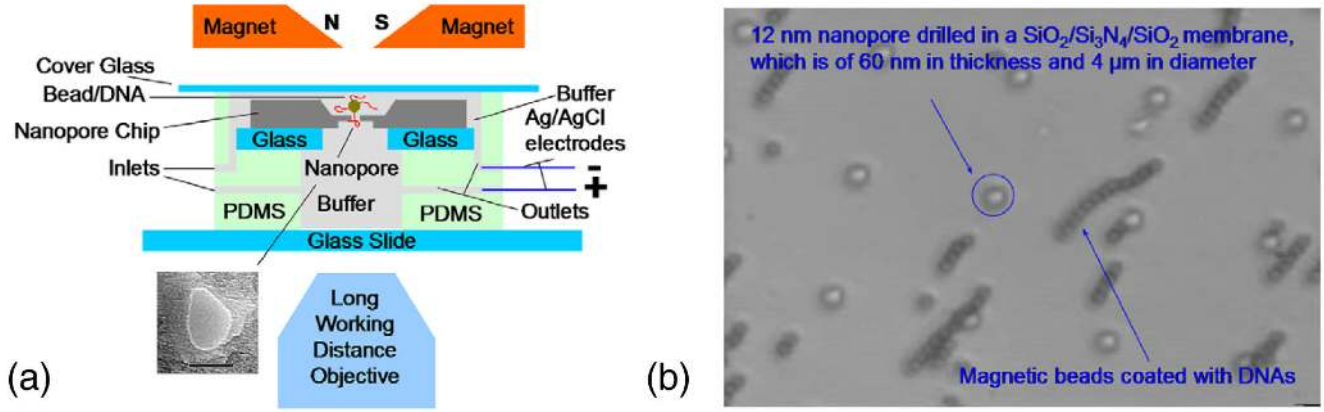

Figure 2.

(a) Schematic of the experimental setup. The fluidic cell is sitting between a long working distance objective and the magnetic tweezers. The fluidic cell is made of glass slides, PDMS, and cover glass, with inlets and outlets for both the upper chamber and the bottom chamber. The two chambers are separated by a nanopore chip with the pore diameter 12 nm (the scale bar in the TEM image is 10 nm). (b) Video image of nanopore membrane and DNA-coated magnetic beads.

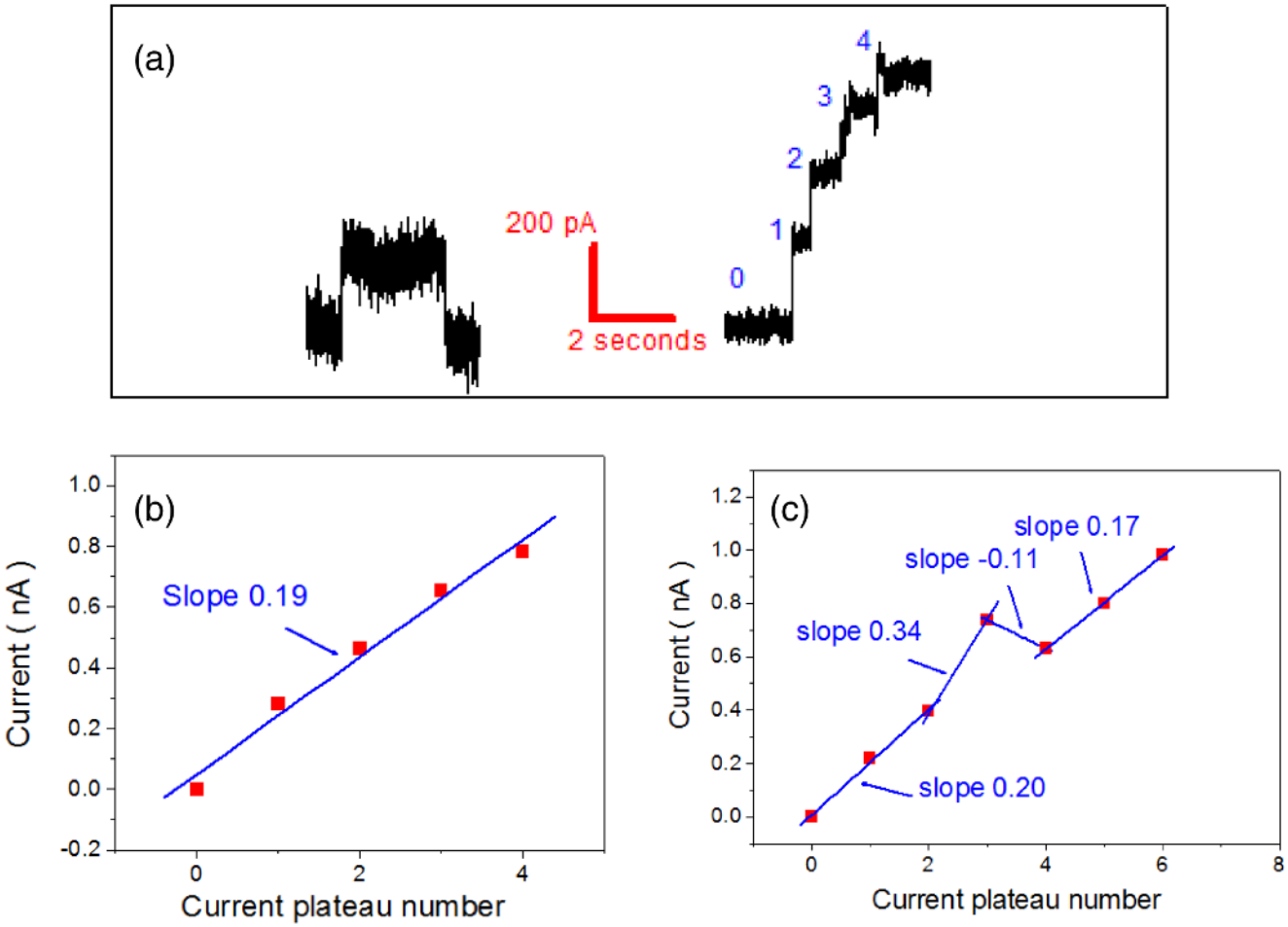

Figure 3.

(a) Time trace of ionic current through a 20 nm nanopore at 200 mV bias and 0.1 M KCl. Red scale bars show the timescale and the ionic current scale. The left panel shows that the ionic current increases and then drops back to the baseline level and the right panel shows stepwise ionic current increases. Note that this stepwise ionic current increase is a very rare event. (b) The ionic current plateaus labeled in (a) versus the label number (the baseline current when there is no DNA in the nanopore is subtracted). It shows that four DNAs were captured into the nanopore. (c) The ionic current plateaus versus the label number for another nanopore (the baseline current when there is no DNA in the nanopore is subtracted). It shows that two DNAs and a folded DNA were captured into the nanopore, then the free end of the folded DNA passed through the nanopore, then another two DNAs were captured into the nanopore.
(This figure is in colour only in the electronic version)

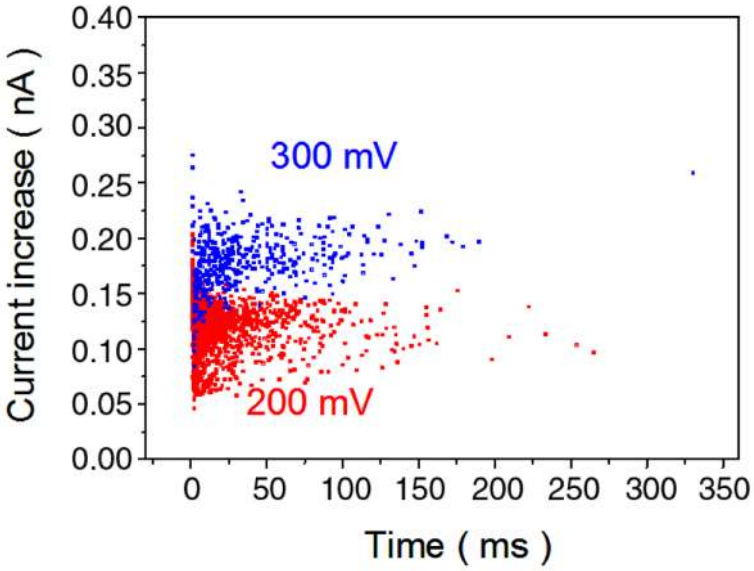

Figure 4.

The amplitudes of the current changes for DNA captures versus capture time at voltage bias 200 mV (shown in red) and 300 mV (shown in blue) respectively (7×10 nm^2 pore at 0.1 M KCl buffer).

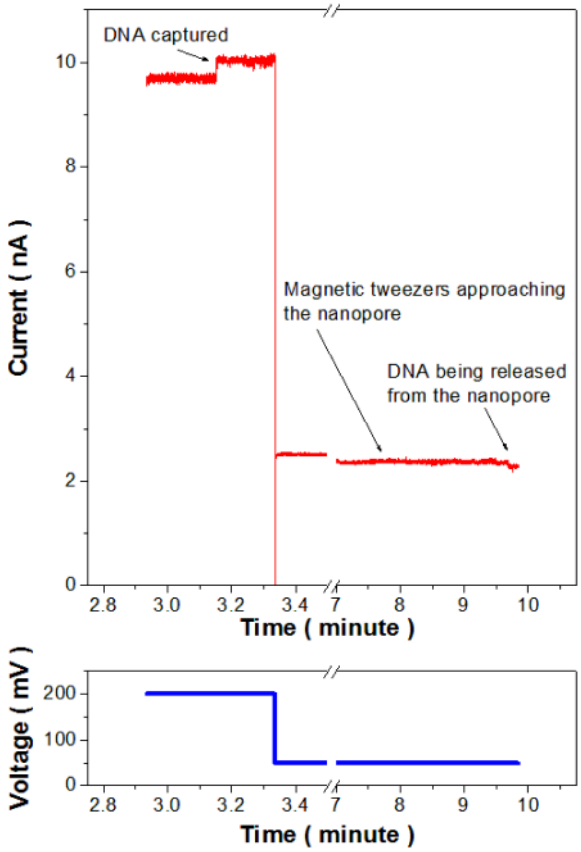

Figure 5.

Nanopore-magnetic tweezers experiment. Top panel: ionic current through a 10 nm SiO_2 pore as a function of time (arbitrary start). Lower panel: applied voltage across the nanopore device as a function of time. The voltage is set at 200 mV at the beginning, and then set to 50 mV after a DNA is captured into the nanopore. The magnetic tweezers is driven towards the nanopore chip by a nanopositioning stage until the DNA is released from the nanopore, indicated by an ionic current drop. The current mismatch between $t = 3.5$ and 7 min is due to the slow drift of the ionic current. (The slow drift of baseline current of SiO_2 or Si_3N_4 pores is a well-known but poorly understood phenomenon. It is generally attributed to the surface chemistry [48] of the SiO_2 or Si_3N_4 surfaces in buffer conditions or air bubbles [49] being trapped or released from the surface of the nanopore.)

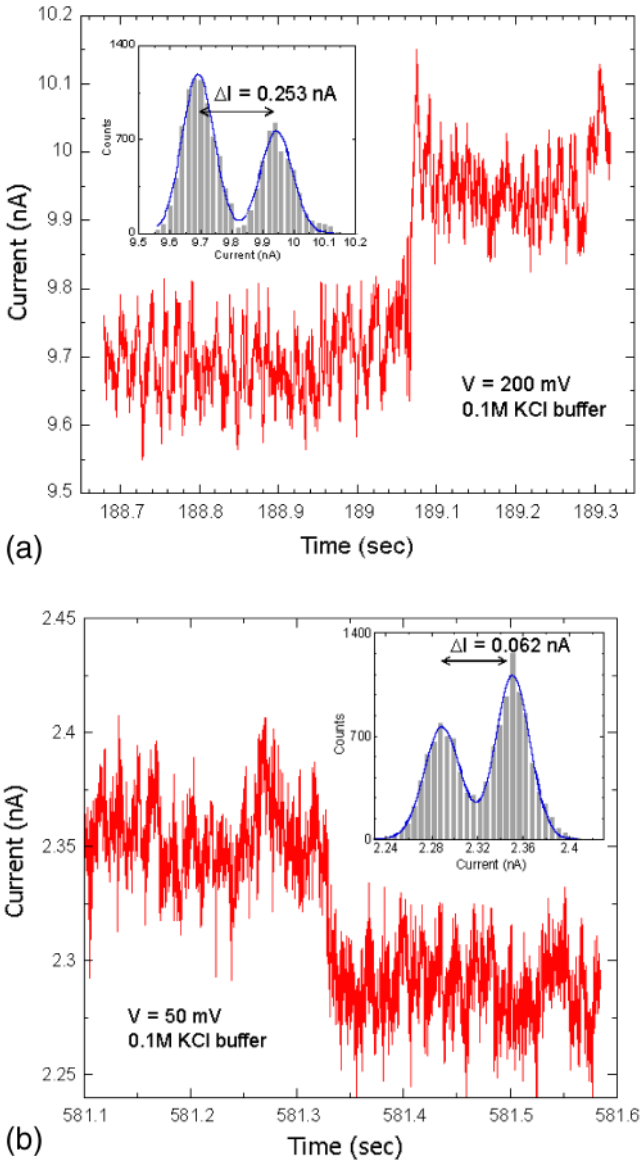

Figure 6.

Ionic current trace of DNA being captured and being released. (a) Capture of a DNA into the nanopore at 200 mV bias voltage across the pore. (b) DNA being released from the nanopore at 50 mV bias voltage across the pore. The inset in each figure shows the histogram of the corresponding ionic current trace. The histograms are fit by a sum of two Gaussian functions.

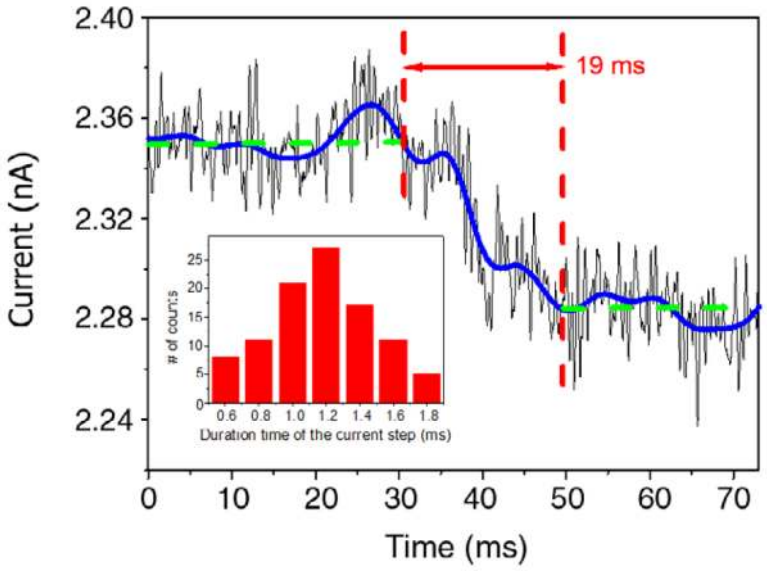

Figure 7.

Estimating the time of DNA release from the nanopore. A zoom-in of the time trace of the nanopore ionic current as the DNA is being pulled out of the nanopore by magnetic force. (Note $t = 0$ is re-defined.) The thick blue line is a smoothed curve of the same data. Green lines are corresponding to the two peaks of the double Gaussian fit shown in the inset of figure 6(b). For comparison, the inset shows the histogram of the transitional times of ionic current increases and decreases from 50 sequential events (DNA is captured into the nanopore and then released from the nanopore due to breakage of streptavidin–biotin bond). Note that the peak at 1.2 ms in the inset is not the actual time that the end of the DNA passes through the nanopore. It is due to the 1 kHz cutoff frequency set in the ionic current measurement system.